

1 **Morphospecies-dependent disaggregation of colonies of the**
2 **cyanobacterium *Microcystis* under high turbulent mixing**

3
4 Ming Li^{1,2,#,*}, Man Xiao^{3,4,#}, Pei Zhang^{5,6}, David P Hamilton³

5 ¹College of Natural Resources and Environment, Northwest A & F University, Yangling
6 712100, PR China

7 ²Collaborative Innovation Center of Water Security for Water Source Region of Mid-line
8 of South-to-North Diversion Project, Nanyang Normal University, Nanyang, 473061, PR
9 China

10 ³Australian Rivers Institute, Griffith University, Nathan, QLD 4111, Australia

11 ⁴School of Environment, Griffith University, Nathan, QLD 4111, Australia

12 ⁵State Key Laboratory of Hydrology-Water Resources and Hydraulic Engineering, Hohai
13 University, Nanjing, 210098, PR China

14 ⁶School of Civil Engineering, University of Queensland, St Lucia, QLD 4072, Australia

15 # These authors contributed equally. The authors declare no conflict of interest.

16 ***Correspondence**

17 Phone: 86+029-87080055

18 Fax: 86+029-87080055

19 Email: lileaf@163.com; lileaf@nwsuaf.edu.cn

20 **Abstract**

21 Preventing formation of large colonies and reducing colony size of the cyanobacterium
22 *Microcystis* may lead to reductions in bloom formation. Here we investigated the effects
23 of artificial mixing on morphology and disaggregation dynamics of *Microcystis* colonies
24 in vivo, using a stirring device and a laser particle analyzer. The turbulent dissipation rate
25 (ϵ) was varied from 0.020 to 0.364 m² s⁻³. We hypothesized that colonies of
26 *M. aeruginosa* and *M. ichthyoblabe* would be more susceptible to disaggregation from
27 turbulent mixing than colonies of *M. wesenbergii*. Our results showed that colony size of
28 *M. aeruginosa* and *M. ichthyoblabe* decreased with increased turbulence intensity and
29 duration of stirring for $\epsilon > 0.094$ m² s⁻³, while *M. wesenbergii* showed less obvious
30 changes in colony size with mixing. Spherical *M. wesenbergii* colonies exposed to high
31 turbulence intensities for 30 min gradually transitioned to colony morphologies similar to
32 *M. ichthyoblabe* and *M. aeruginosa*-like colonies (irregular, elongated or lobed, with
33 distinct holes). Our results suggest that turbulent mixing is an important factor driving
34 morphological changes of *Microcystis* colonies, and artificial mixing may effectively
35 reduce colony size of *Microcystis*, thereby preventing bloom formation.

36 **Keywords:** artificial mixing; colony formation; turbulent dissipation rate; Kolmogorov
37 scale; *Microcystis*; morphospecies

38 **Introduction**

39 Size and morphology of cyanobacteria, particularly colony formation, critically affect
40 grazing pressure by zooplankton, migration velocities, and nutrient uptake (Xiao et al.
41 2018). They determine whether populations are entrained into the prevailing mixed layer
42 turbulence or become buoyant, which is often associated with surface bloom formation
43 (Oliver et al. 2012, Wallace et al. 2000).

44 *Microcystis* is a genus of cyanobacteria with high phenotypic plasticity. It exists mostly
45 as single cells under laboratory culture conditions (Li et al. 2013, Yang et al. 2008), but
46 can form surface ‘scums’ consisting of large colonies (100 – 2000 µm) in the field (Rowe
47 et al. 2016, Zhu et al. 2014). Colony size and morphology determine the vertical floating
48 velocity of *Microcystis* colonies and whether colonies can dis-entrain from turbulent
49 mixing to float up towards the water surface and form blooms (Wallace et al. 2000). The
50 floating velocity is usually described by Stoke's Law, based on density, colony size, and
51 morphology (termed the shape coefficient). These three variables differ widely amongst
52 *Microcystis* morphospecies (Li et al. 2016).

53 Artificial mixing in the laboratory is highly effective in disaggregating colonies of
54 *Microcystis* but most work has been limited to examining particular morphospecies, i.e.,
55 *M. aeruginosa* (O'Brien et al. 2004, Regel et al. 2004). Morphospecies such as
56 *M. wesenbergii*, *M. flos-aquae*, *M. ichthyoblabe* and *M. aeruginosa* may dominate in
57 natural eutrophic systems and often undergo successional sequences in these systems (Jia
58 et al. 2011, Ozawa et al. 2005, Park et al. 1993, Yamamoto and Nakahara 2009, Zhu et al.
59 2016). Based on spatial distributions of *Microcystis* morphospecies, Otten and Paerl
60 (2011) deduced that colonies of *M. aeruginosa* and *M. ichthyoblabe* are more susceptible

61 to wind shear than those of *M. wesenbergii* and *M. flos-aquae*. Disaggregation of
62 *Microcystis* colonies at the morphospecies level, however, has not been systematically
63 investigated or quantified.

64 Colony morphology of *Microcystis* changes when mucilage surrounding the colonies is
65 dissolved (Li et al. 2014b). The process of mucilage dissolution might also be accelerated
66 by mixing. Thus, the interactions of mixing, colony morphology and physiological status
67 of *Microcystis* are likely to have a key regulatory role in bloom formation. In this study
68 our primary objective was to quantify the effects of turbulent mixing, using artificial
69 stirring on morphological changes and colony disaggregation of three *Microcystis*
70 morphospecies.

71

72 **Material and methods**

73 **Collection of *Microcystis* colonies**

74 *Microcystis* colonies were collected from Meiliang Bay (31°24'–31°28'N, 120°10'–
75 120°12'E) in Lake Taihu, China. This bay is located in the northern part of Lake Taihu
76 where frequent and severe *Microcystis* blooms have occurred over the last two decades
77 (Duan et al. 2009). *Microcystis* colonies were sampled on 2 July, 7 September and 15
78 October 2014, when three distinct morphospecies could be distinguished:
79 *M. ichthyoblabe*, *M. wesenbergii* and *M. aeruginosa*. Colonies were gently filtered
80 through sieves of different pore sizes into three size groups, representing small, medium
81 and large colonies (Fig. S1). The three size groups corresponded to different colony sizes
82 of *Microcystis* morphospecies: Colonies of *M. ichthyoblabe* were divided into < 212, 212
83 – 300 and > 300 µm, indicative of small, medium and large sized groups, *M. wesenbergii*

84 into < 300, 300 – 500 and > 500 μm , and *M. aeruginosa* into < 500, 500 – 600 and > 600
85 μm .

86

87 **Experimental setup**

88 The mixing experiment was carried out using a laser particle analyzer (Mastersizer
89 2000 Particle Size Analyzer, Malvern Instruments, Ltd). The propeller has three blades
90 and was set 15 mm above the bottom of a 500 mL beaker (Fig. 1a). The propeller was
91 connected to the analyzer with a pump to mix the media in the beaker during the
92 experiment (Fig. 1a). The propeller was set at rotation speeds of 600, 800, 1000, 1200,
93 1400 and 1600 rpm, and run for 30 min at each speed. From preliminary experiments, a
94 rotation speed of 600 rpm was found through trial and error to produce minimal
95 disaggregation of *Microcystis* colonies of all the three morphospecies, and 1600 rpm
96 produced significant disaggregation without visible air bubbles.

97 For each group of mixing experiments, background measurements were firstly
98 conducted using 450 mL of tap water in the beaker without added *Microcystis* colonies
99 (Fig. 1a). Thereafter, the three size groups of the three *Microcystis* morphospecies were
100 gently mixed into the beaker for measurements of colony size distribution. Measurements
101 started when the obscuration parameter of particle size analyzer, which reflects
102 concentration of colonies in the beaker, reached 15%. Here, the obscuration value of 15%
103 was chosen because it is the optimal concentration for the laser particle analyzer to pick
104 up the size distribution. The values of intrinsic refractive index (n) and absorption of light
105 by the particle (k) by the laser particle analyzer were set to 1.40 and 0.1, based on
106 extensive tests conducted by Li et al. (2014b).

107 The distribution of colony sizes was measured by laser particle analyzer every 2 min.
108 D_{50} of each sample was used to assess variation in colony size, defined as the diameter
109 where 50% of the total biovolume is below this size. After 30 min of mixing, the treated
110 samples were collected for microscopic observation and compared with samples not
111 subjected to mixing.

112

113 **Calculation of turbulent dissipation rates and Kolmogorov scale**

114 A modified Discrete Element Lattice Boltzmann Method (DELBM) was used to
115 simulate mixing intensity during the mixing experiment. DELBM is a relatively new
116 computational fluid dynamics (CFD) method used to delineate fluid structure and fluid-
117 particle interactions (Galindo Torres et al. 2016, Galindo-Torres 2013, Zhang et al. 2017,
118 Zhang et al. 2016). The model has been validated in similar studies of rigid object-fluid
119 interactions (Galindo Torres et al. 2016, Zhang et al. 2016). The main advantage of this
120 model is its ability to efficiently and accurately resolve the momentum exchanges
121 between rigid, irregularly shaped objects and the fluid, without re-meshing (Galindo-
122 Torres 2013, Galindo-Torres et al. 2012). A Smagorinsky subgrid turbulence module was
123 employed to simulate at high Reynolds numbers, using a Smagorinsky constant set to
124 0.14 (Galindo-Torres 2013, Zhang et al. 2016).

125 For DELBM simulations, the shape of propeller is described by a three-dimensional
126 polygon mesh, where the impeller is resolved using a Computed Tomography (CT) scan
127 to minimize error in the numerical representation of the propeller shape. The original
128 very fine mesh from the CT scan was reduced to a coarser resolution (see Fig. 1b – g)
129 without losing the general shape of the propeller, based on preliminary simulations. Two

130 grid resolutions (88×88×110 and 176×176×220) for the beaker were tested to check the
131 independence of simulations on the grid resolution, i.e., the difference between the two
132 resolutions were found negligible. Thus, the grid resolution and the time step were set to
133 1×10^{-3} m and 5×10^{-5} s, respectively, and approximately 850,000 lattices were used to
134 represent the beaker in the simulation. The relaxation parameter, which is a dimensionless
135 parameter dependent only on the viscosity, was set to 0.500015 corresponding to the
136 viscosity of water at room temperature during the mixing experiment.

137 Values of total turbulent kinetic energy (TKE, $\text{m}^2 \text{s}^{-2}$), turbulent dissipation rate (ϵ , m^2
138 s^{-3}) and Kolmogorov scale (μm) determined from DELBM simulations are given for each
139 mixing speed (Table 1). The calculation of ϵ depends on the average velocity, which is
140 determined from steady state simulations. Therefore, all simulations at each speed were
141 run to steady state, indicated by the magnitude of the dimensionless velocity, as shown in
142 Fig. 1b–g. Our simulated results of TKE, ϵ , and Kolmogorov scale were similar to those
143 measured in Xiao et al. (2016), which the stirring device and range of rotation speeds
144 were employed similarly to our study.

145

146 **Measurement of colony size and morphospecies**

147 For each mixing experiment, the size and morphospecies of *Microcystis* colonies were
148 analyzed by taking photomicrographs using an Olympus C-5050 digital camera coupled
149 to an Olympus CX31 optical microscope. The photomicrographs were analyzed using the
150 UTHSCSA ImageTool v3.00 software (Department of Dental Diagnostic Science,
151 University of Texas Health Science Center, San Antonio, TX, USA). A minimum of 200
152 colonies per sample was analyzed to calculate the percentage of biovolume of various

153 morphospecies for each size group of each morphospecies (*M. ichthyoblabe*,
154 *M. aeruginosa* and *M. wesenbergii*). *Microcystis* morphospecies were identified
155 following the taxonomic methods of Yu et al. (2007). Only the classical spherical
156 *M. wesenbergii* colonies were identified as *M. wesenbergii* as shown in Fig. 4e. The
157 irregularly branched spherical colonies with no visible mucilage were considered a
158 transitional morphological form of *M. wesenbergii*. The reticulated colonies with visible
159 margins were categorized as reticular *M. wesenbergii*. The biovolume of individual
160 colonies was calculated assuming they were spherical. This approximation was applied
161 because currently there are no reliable methods to accurately measure and calculate the
162 diameter of *Microcystis* colonies, especially those with irregular morphologies. The
163 length and width of colonies were measured directly from the longest axis (length) and
164 the shortest axis (width, aligned perpendicular to the longest axis). The diameter of
165 *Microcystis* colonies was calculated as $\text{diameter} = (\text{length} \times \text{width})^{1/2}$ (Li et al. 2014a).

166

167 **Results**

168 **Effects of turbulence on disaggregating *Microcystis* colonies**

169 The effects of turbulent mixing on disaggregation of *Microcystis* colonies differed
170 substantially, depending on morphospecies, mixing intensity and mixing duration (Fig. 2).
171 *M. ichthyoblabe*, which has tightly packed cells, was most easily disaggregated (Fig. 2a,
172 d, g), followed by *M. aeruginosa* (Fig. 2c, f, i) and *M. wesenbergii* (Fig. 2b, e, h).
173 *M. ichthyoblabe* colonies were not affected at the lowest mixing intensity ($\epsilon = 0.02 \text{ m}^2 \text{ s}^{-3}$),
174 but the D_{50} (where 50% of the total biovolume is below this size) of the three size
175 groups all decreased sharply to approximately 75% of the initial value after 30-min

176 mixing at ε of $0.094 \text{ m}^2 \text{ s}^{-3}$ (Fig. S1). At the maximum ε of $0.364 \text{ m}^2 \text{ s}^{-3}$, D_{50} of
177 *M. ichthyoblabe* colonies from all three size groups decreased to $< 100 \text{ }\mu\text{m}$ after 10-min
178 mixing and to $< 40 \text{ }\mu\text{m}$ after 30-min mixing. In comparison, for ε of $0.094 \text{ m}^2 \text{ s}^{-3}$ there
179 was little disaggregation of *M. aeruginosa* colonies, which has elongated morphology
180 and distinct holes. The D_{50} decreased to about 75% of the initial value for ε of 0.364 m^2
181 s^{-3} after 30-min mixing. Colonies of *M. wesenbergii*, which are spherical and elongated
182 with a visible outer colony margin, barely disaggregated under any of the mixing
183 intensities, irrespective of the initial colony size.

184 The final colony size of all *Microcystis* morphospecies always decreased with
185 decreasing Kolmogorov scale values calculated from the mixing intensities. Nevertheless,
186 only *M. ichthyoblabe* colonies could be disaggregated to the minimum size after 30-min
187 mixing at a dissipation rate ε of $0.364 \text{ m}^2 \text{ s}^{-3}$ (Fig. 3a, d, g). In addition, for all the three
188 morphospecies, the large size group was more susceptible to turbulent mixing than the
189 small size group (Fig. 3).

190

191 **Changes in colonial morphology induced by turbulence**

192 Colonies of *M. ichthyoblabe*, *M. aeruginosa* and *M. wesenbergii* all underwent
193 morphological changes after 30 min under all six mixing intensities (Fig. 4).
194 *M. ichthyoblabe* colonies changed from a loosely assembled outer mass with tightly
195 packed inner cells (Fig. 4a) to smaller and tightly packed masses (Fig. 4b). *M. aeruginosa*
196 colonies had the least visible morphological changes with mixing, and remained irregular
197 with lobes, distinct holes and irregular shapes (Fig. 4c, d). *M. wesenbergii* colonies
198 transitioned gradually from initially spherical or elongated morphology with visible outer

199 margins which retained mucilage (Fig. 4e) to reticular forms (Fig. 4f), and then to forms
200 with distinct holes and weakly resolved colony margin, similar to those of *M. aeruginosa*
201 (Fig. 4g).

202 *M. wesenbergii* colonies transitioned after 30-min mixing to varied proportions of
203 reticular and *M. aeruginosa*-like morphologies, depending on mixing intensities and
204 initial colony sizes (Fig. 5). The incidence of spherical *M. wesenbergii* colonies decreased
205 from about 90% to 55%, 50% and 20% at ϵ of $0.364 \text{ m}^{-2} \text{ s}^{-3}$ for small (Fig. 5a), medium
206 (Fig. 5b) and large (Fig. 5c) size groups, respectively. In comparison, at the lower ϵ of
207 $0.02 \text{ m}^{-2} \text{ s}^{-3}$, the incidence of spherical *M. wesenbergii* colonies decreased to 80%, 55%
208 and 50% for each of the three size groups.

209

210 **Discussion**

211 **Turbulent dissipation rate assessment**

212 Our results demonstrate that *M. ichthyoblabe* and *M. aeruginosa* colonies could be
213 potentially disaggregated by high turbulent mixing, while *M. wesenbergii* colonies
214 showed little disaggregation, even at ϵ approaching five orders of magnitude higher than
215 the highest values measured in deep lakes ($10^{-11} - 10^{-6} \text{ m}^2 \text{ s}^{-3}$) (Wüest and Lorke 2003).
216 The turbulent dissipation rate in Lake Taihu, a large, shallow lake in Jiangsu province,
217 China with a mean depth of 2 m, was reported to range from 6.014×10^{-8} to $2.389 \times 10^{-4} \text{ m}^2$
218 s^{-3} (Zhou et al. 2016). The maximum value *in situ* was approximately one-tenth of the
219 minimum value employed in the current study. The investigations by Zhou et al. (2016)
220 were conducted in the field using an acoustic Doppler velocimeter, with sampling unable
221 to be conducted on very windy days. MacKenzie and Leggett (1993) described turbulent

222 dissipation rate as a function of wind speed in aquatic environments:

$$223 \quad \varepsilon = 5.82 \times 10^{-6} w^3 / h \quad (1)$$

224 where w is wind speed (m s^{-1}) and h is the water depth (m). From this equation,
225 considering the depth of Lake Taihu as 2 m, the wind speed during the field investigation
226 by Zhou et al. (2016) may be in the range 0.275 to 4.35 m s^{-1} . Measured wind speeds in
227 Lake Taihu can be 5.5 to 10.7 m s^{-1} for 32.6% of the time and 10.8 to 17.1 m s^{-1} for 1.22%
228 of time (Wang et al. 2016). Since the turbulent dissipation rate increases with the wind
229 speed, the upper limit of dissipation rate in shallow lakes such as Lake Taihu may be
230 much higher than the reported value of $2.389 \times 10^{-4} \text{ m}^2 \text{ s}^{-3}$. Theoretically, the minimum
231 turbulent dissipation rate used in the current study ($0.020 \text{ m}^2 \text{ s}^{-3}$) could almost equate to a
232 wind speed of 19.0 m s^{-1} in Lake Taihu, which was slightly higher than the maximum
233 reported wind speed in Lake Taihu (17.1 m s^{-1} ; Wang et al. 2016). In the absence of
234 turbulent dissipation rates recorded at very strong wind speeds, we assumed that the
235 minimum value of turbulent dissipation rate in the current study was similar to that of
236 Lake Taihu under extreme wind conditions, such as a typhoon.

237 Although artificial mixing by aeration, diffusers or pumping devices has been on
238 occasions used to control cyanobacterial blooms in many lentic systems, turbulent
239 dissipation rates in these systems have not been quantified (Visser et al. 2016). Visser et
240 al. (1996) demonstrated successful control of cyanobacterial blooms in Lake Nieuwe
241 Meer (30 m in depth) with an aeration system. They illustrated that the aeration decreased
242 the temperature to $< 2 \text{ }^\circ\text{C}$ between the water surface and bottom of the lake. In another
243 30-m deep lake, Vlietland in the Netherlands, a wind speed of 12 m s^{-1} was found to
244 result in similar levels of density stratification, with *Microcystis* colonies distributed

245 throughout the water depth (Aparicio Medrano et al. 2013). The turbulent dissipation rate
246 of the artificial mixing used in Lake Nieuwe Meer could be deduced from Eq. (1) to be
247 $3.35 \times 10^{-4} \text{ m}^2 \text{ s}^{-3}$. This dissipation rate is similar to the maximum value reported in Lake
248 Taihu with a wind speed of approximately 4.87 m s^{-1} . Therefore, these artificial mixing
249 devices may potentially partially mix down buoyant surface colonies of *Microcystis* spp.
250 but may not necessarily break up the colonies in a way that occurs with very high
251 dissipation rates occurring in shallow lakes under extreme wind conditions or using our
252 laboratory stirring device.

253 Laboratory studies have frequently used an oscillating grid and churn-dasher to induce
254 turbulent mixing. The former device has produced mixing with ϵ in the range 10^{-9} to 10^{-6}
255 $\text{m}^2 \text{ s}^{-3}$ (O'Brien 2003, Wilkinson et al. 2016), while the later device has generated mixing
256 with ϵ up to $0.313 \text{ m}^2 \text{ s}^{-3}$ (Hondzo et al. 1997) and $0.080 \text{ m}^2 \text{ s}^{-3}$ (Xiao et al. 2016),
257 respectively. The ϵ induced in the stirring device of the current study was the same order
258 of magnitude as the values reported in the churn-dasher. Nevertheless, these unrealistic
259 values are not necessarily representative of natural systems.

260

261 **Disaggregation of *Microcystis* colonies by turbulence**

262 Under the artificial mixing rates used in this study, colony disaggregation of
263 *Microcystis* morphospecies was in the order of *M. ichthyoblabe* > *M. aeruginosa* >
264 *M. wesenbergii*. Our order differs from that deduced by Otten and Paerl (2011) because
265 they ranked the spherical colonies, which have tightly arranged cells and no surrounding
266 gelatinous envelope, as hardest to break. These authors categorized the spherical colonies
267 as *M. flos-aquae*, while we considered they were *M. ichthyoblabe*, the easiest to

268 disaggregate under mixing. Consistently, however, *M. wesenbergii* colonies had the
269 highest resistance to turbulence. This is because, unlike *M. ichthyoblabe* and
270 *M. aeruginosa*, *M. wesenbergii* colonies have a clearly distinguishable gelatinous
271 envelope which is composed of pectin-like extracellular polysaccharides (EPSs). Capel et
272 al. (2006) found that during the gelling process of pectin, the shear strength of pectin and
273 pectin-like EPS increased. Thus, the gelatinous envelope encapsulating *M. wesenbergii*
274 colonies appears to be important in conferring resistance to turbulence.

275 In a previous cyanobacterial mixing experiment by O'Brien et al. (2004) using a grid-
276 stirred tank, the initial D_{50} of *M. aeruginosa* colonies was about 400 μm , which is similar
277 to that of the smallest size group of *M. aeruginosa* in our current study (Fig. 3c). O'Brien
278 et al. (2004) found the maximum stable colony diameter was from 220 to 420 μm , which
279 is also similar to the range of 300 to 400 μm measured in our experiments after 30 min of
280 mixing. The maximum dissipation rate used by O'Brien et al. (2004) was $9 \times 10^{-5} \text{ m}^2 \text{ s}^{-3}$,
281 which is however, three orders of magnitude less than our minimum value. One reason
282 for their much lower dissipation rate might be that measurements were outside of the
283 stirred grid where the values are likely to be considerably smaller. *Microcystis* colonies
284 used in our study were collected from large, wind-exposed lakes. The colonies collected
285 from a small, sheltered pond (O'Brien et al. 2004) may be more susceptible more fragile
286 and prone to disaggregation with turbulent mixing.

287 This study showed that colonies of *M. ichthyoblabe* are more fragile than those of
288 *M. aeruginosa* and *M. wesenbergii*. The smallest colony size of *M. ichthyoblabe* was
289 around 40 μm , similar to the Kolmogorov scale, at the highest turbulent dissipation rate
290 of $0.364 \text{ m}^2 \text{ s}^{-3}$. Therefore, at ε of $0.364 \text{ m}^2 \text{ s}^{-3}$, *M. ichthyoblabe* colonies had been fully

291 disaggregated to their minimum size and any additional turbulent kinetic energy would be
292 dissipated into heat (Peters and Marrasé 2000). Mixing with ϵ of $0.020 \text{ m}^2 \text{ s}^{-3}$, i.e., four
293 orders of magnitude higher than the largest values measured in deep lakes (Wüest and
294 Lorke 2003), had little disaggregating effect on *M. ichthyoblabe* colonies. Our results
295 indicate that large colonies are not as fragile as has been postulated (e.g., (Otten and Paerl
296 2011)) and colony morphology associated with differences in *Microcystis* morphospecies
297 may be more significant than colony size *per se*.

298 The impellers in our mixing device may break down the colonies directly. However,
299 Fig. 3a illustrates that the minimum size of disaggregated colonies was similar to the
300 Kolmogorov scale (μm), suggesting that the main disaggregating effect is from the
301 mixing but not directly from the impellers. The decrease in D_{50} of the colonies with time
302 appears to follow an exponential decay, suggesting a first order kinetic reaction. This
303 reaction suggested that the decrease rate of D_{50} was a constant at each dissipation rate.

304

305 **Changes in colony morphology induced by turbulence**

306 Our experiment also illustrated that the tightly packed cells in *M. ichthyoblabe*
307 colonies were easily disaggregated into smaller colonies comprised of loosely bound cells.
308 *M. flos-aquae* has sometimes been recognized as a morphotype of *M. ichthyoblabe*; a
309 taxonomic classification also noted by Watanabe (Watanabe 1996). Any changes in
310 colony morphology of *M. aeruginosa* exposed to turbulence were not recognizable in the
311 current study.

312 *M. wesenbergii* has been found to be morphologically and genetically distinct from
313 other *Microcystis* morphospecies, e.g., *M. aeruginosa*, *M. flos-aquae*, and

314 *M. ichthyoblabe*, based on 16S-23S rDNA-ITS sequences (Otten and Paerl 2011) or gene
315 *cpcBA*-IGS (Tan et al. 2010). However, Xu et al. (2016) found a contradictory result
316 from the high homozygosity in sequences of 16S-23S and *cpcBA*-IGS in a range of
317 *Microcystis* samples except for one *M. aeruginosa* colony. It appears to be extremely
318 difficult to identify different *Microcystis* morphospecies using molecular tools, such as
319 16S rDNA (Harke et al. 2016, Otsuka et al. 1998, Xu et al. 2014), 16S-23S rDNA
320 (Otsuka et al. 1999, Xu et al. 2016), genomic DNA homologies (Otsuka et al. 2001) or
321 fatty acid analysis (Le Ai Nguyen et al. 2012). These studies all indicate morphology of
322 *Microcystis* colonies changes under different environmental conditions and that classical
323 taxonomic studies should still be used to complement modern molecular techniques.

324 Spherical *M. wesenbergii* colonies gradually transformed to reticular *M. wesenbergii*-
325 like colonies and then *M. aeruginosa*-like colonies in our experiment. The reticular
326 *M. wesenbergii* colonies have been identified as *M. aeruginosa* when the distinguishable
327 gelatinous envelope is solubilized with EPS (Otsuka et al. 2000). Li et al. (2014b)
328 suggested that solubilisation of mucilage induces changes in colony morphology resulting
329 in transitions from *M. wesenbergii* to *M. aeruginosa*. A conceptualization of our
330 hypothesis regarding changes in colonial morphology from *M. wesenbergii* to
331 *M. aeruginosa* is shown in Fig. 6. Turbulent mixing induces spherical *M. wesenbergii*
332 colonies to change into reticular *M. wesenbergii*-like colonies, and the further
333 solubilisation of mucilage removes the distinguishable gelatinous envelope, resulting in
334 *M. aeruginosa*-like colonies. The phenomenon of mucilage solubilisation was described
335 previously as a dilution process of polysaccharide in the mucilage with time (Li et al.
336 2014b, Xiao et al. 2018).

337 *M. wesenbergii* has been considered as a unique species in the *Microcystis* genera at
338 both phenotypic and genetic level (Otten and Paerl 2011). Our results suggest that
339 *Microcystis* can change spontaneously from *M. wesenbergii* colonies into *M. aeruginosa*-
340 like colonies under mixing. This observation might explain the absence of sequence-
341 based differences in morphospecies (Otsuka et al. 1998, 1999, Otsuka et al. 2001, Tan et
342 al. 2010, Xu et al. 2014, Xu et al. 2016).

343

344 **Artificial mixing to control blooms by reducing *Microcystis* colony size**

345 Reducing colony size of *Microcystis* has been considered as a possible method to
346 prevent occurrence of *Microcystis* blooms (Zhu et al. 2016). Our results showed that
347 artificial mixing significantly reduced colony size of *M. ichthyoblabe* but not that of
348 *M. wesenbergii* or *M. aeruginosa*. In many freshwater systems, such as Lakes Taihu,
349 Chaohu (China), Suwa (Japan) and Biwa (Japan), *M. ichthyoblabe*, *M. wesenbergii* and
350 *M. aeruginosa* sequentially dominate from late spring to late autumn (Jia et al. 2011,
351 Ozawa et al. 2005, Park et al. 1993, Yamamoto and Nakahara 2009, Zhu et al. 2016). This
352 seasonal succession provides a period when *M. ichthyoblabe* dominates phytoplankton
353 biomass and artificial mixing could be applied to disaggregate *M. ichthyoblabe* colonies.
354 Our experiment showed that for a turbulent dissipation rate of $0.364 \text{ m}^2 \text{ s}^{-3}$, D_{50} of
355 *M. ichthyoblabe* colonies was $< 100 \text{ }\mu\text{m}$ after 10 min of mixing and $< 40 \text{ }\mu\text{m}$ after 30 min
356 of mixing. Zhu et al. (2014) suggested that if colony size of *Microcystis* is $< 100 \text{ }\mu\text{m}$ in
357 Lake Taihu, blooms would not occur as the small colonies would be unable to disentrain
358 from the wind induced mixing. Hence, continuous artificial mixing at dissipation rates of
359 $0.364 \text{ m}^2 \text{ s}^{-3}$ for 10 min could effectively reduce *Microcystis* colony sizes, and may be

360 most effective at a time when *M. ichthyoblabe* dominates.

361 Artificial mixing has successfully reduced *Microcystis* blooms in several lakes, such as
362 Nieuwe Meer in The Netherlands (Jungo et al. 2001, Visser et al. 1996), Lake Dalbang in
363 South Korea (Heo and Kim 2004) and Bleioch Reservoir in Germany (Becker et al. 2006).
364 It mixes *Microcystis* colonies to deeper layers and induces greater light limitation. In
365 other cases, however, artificial mixing has failed to control blooms (Jöhnk et al. 2008,
366 Lilindenschmidt 1999, Tsukada et al. 2006), and this may be related to the morphospecies
367 present, the mixing regime used (continuous mixing or intermittent pulses), and the
368 duration of mixing (Visser et al. 2016). Our study sheds new light on why failures may
369 have occurred and it allows for *a priori* assessment of the design requirements for
370 implementation of an effective artificial mixing system. Besides colony formation, over-
371 buoyancy of colonies also plays an important role in the occurrence of *Microcystis*
372 blooms (Ibelings et al. 1991). The buoyancy of *Microcystis* colonies has been attributed
373 to formation of intra-cellular gas vesicles (Pfeifer 2012) and intra-colony gas bubbles
374 (Aparicio Medrano et al. 2013). Both gas vesicles and bubbles may be destroyed
375 physically (Zhang et al. 2006). So far, what governs the actual size of colonies is still
376 unknown. Thus, artificially reducing colony size of *Microcystis* should also be considered
377 in freshwater management, as well as controlling the over-buoyancy of *Microcystis*
378 colonies.

379

380 **Conclusions**

381 This study quantified the morphological change and disaggregation of colonies of three
382 *Microcystis* morphospecies to a range of mixing intensities, and sheds new light on

383 buoyancy and succession of these morphospecies. Disaggregation of *Microcystis* colonies
384 in response to turbulence varied with morphospecies, ranking in the order of
385 *M. ichthyoblabe* > *M. aeruginosa* > *M. wesenbergii*. At laboratory induced dissipation
386 rates > 0.094 m² s⁻³, *M. ichthyoblabe* colonies disaggregated while *M. wesenbergii* barely
387 changed. The dissipation rates used in the current study are three to four orders of
388 magnitude higher than the measured ranges in deep lakes, however, the very high values
389 are theoretically possible under strong winds or with extremely high rates of artificial
390 mixing. Our mixing experiments portended that wind shear may be expected to have a
391 significant effect only on *M. ichthyoblabe* colonies *in situ*. We also deduced that
392 turbulence induced morphological changes in *Microcystis* colonies related to membrane
393 visibility and porosity of colonies, and membrane integrity should be further investigated
394 under different turbulent regimes using alcian blue dye treatment.

395

396 **Acknowledgements**

397 This work was supported by the National Natural Science Foundation of China [Grant
398 no. 51409216]; the Scientific Research and Service Platform fund of Henan Province
399 (2016151); the Australian Research Council [ARC: linkage project LP130100311]; and a
400 Griffith University Postgraduate International Scholarship. Dr. Ming Li is funded as Tang
401 Scholar by Cyrus Tang Foundation and Northwest A&F University.

402

403 **References**

404 Aparicio Medrano, E., Uittenbogaard, R.E., Dionisio Pires, L.M., van de Wiel, B.J.H. and
405 Clercx, H.J.H. (2013) Coupling hydrodynamics and buoyancy regulation in *Microcystis*

406 *aeruginosa* for its vertical distribution in lakes. Ecol. Modell. 248, 41–56.

407 Becker, A., Herschel, A. and Wilhelm, C. (2006) Biological effects of incomplete
408 destratification of hypertrophic freshwater reservoir. Hydrobiologia 559, 85–100.

409 Capel, F., Nicolai, T., Durand, D., Boulenguer, P. and Langendorff, V. (2006) Calcium
410 and acid induced gelation of (amidated) low methoxyl pectin. Food Hydrocoll. 20, 901–
411 907.

412 Duan, H., Ma, R., Xu, X., Kong, F., Zhang, S., Kong, W., Hao, J. and Shang, L. (2009)
413 Two-decade reconstruction of algal blooms in China's Lake Taihu. Environ. Sci. Technol.
414 43, 3522–3528.

415 Galindo Torres, S., Scheuermann, A. and Ruest, M. (2016) Simulation engine for fluid
416 solid interaction problems and its application to the modelling of air blast hazards in
417 block cave mining, AGU Fall Meeting Abstracts.

418 Galindo-Torres, S. (2013) A coupled Discrete Element Lattice Boltzmann Method for the
419 simulation of fluid-solid interaction with particles of general shapes. Comput Methods
420 Appl Mech Eng 265, 107–119.

421 Galindo-Torres, S., Pedroso, D., Williams, D. and Li, L. (2012) Breaking processes in
422 three-dimensional bonded granular materials with general shapes. Computer Physics
423 Communications 183, 266–277.

424 Harke, M.J., Steffen, M.M., Gobler, C.J., Otten, T.G., Wilhelm, S.W., Wood, S.A. and
425 Paerl, H.W. (2016) A review of the global ecology, genomics, and biogeography of the
426 toxic cyanobacterium, *Microcystis* spp. Harmful Algae 54, 4–20.

427 Heo, W.-M. and Kim, B. (2004) The effect of artificial destratification on phytoplankton
428 in a reservoir. Hydrobiologia 524, 229–239.

429 Hondzo, M.M., Kapur, A. and Lembi, C.A. (1997) The effect of small-scale fluid motion
430 on the green alga *Scenedesmus quadricauda*. *Hydrobiologia* 364, 225–235.

431 Ibelings, B.W., Mur, L.R., Kinsman, R. and Walsby, A. (1991) *Microcystis* changes its
432 buoyancy in response to the average irradiance in the surface mixed layer. *Arch.*
433 *Hydrobiol.* 120, 385–401.

434 Jia, X., Shi, D., Shi, M., Li, R., Song, L., Fang, H., Yu, G., Li, X. and Du, G. (2011)
435 Formation of cyanobacterial blooms in Lake Chaohu and the photosynthesis of dominant
436 species hypothesis. *Acta Ecologica Sinica* 31, 2968–2977.

437 Jöhnk, K.D., Huisman, J.E.F., Sharples, J., Sommeijer, B.E.N., Visser, P.M. and Stroom,
438 J.M. (2008) Summer heatwaves promote blooms of harmful cyanobacteria. *Global*
439 *Change Biol.* 14, 495–512.

440 Jungo, E., Visser, P.M., Stroom, J. and Mur, L.R. (2001) Artificial mixing to reduce
441 growth of the blue-green alga *Microcystis* in Lake Nieuwe Meer, Amsterdam: an
442 evaluation of 7 years of experience. *Water Sci. Technol: Water Supply* 1, 17–23.

443 Le Ai Nguyen, V., Tanabe, Y., Matsuura, H., Kaya, K. and Watanabe, M.M. (2012)
444 Morphological, biochemical and phylogenetic assessments of water-bloom-forming
445 tropical morphospecies of *Microcystis* (Chroococcales, Cyanobacteria). *Phycological Res.*
446 60, 208–222.

447 Li, M., Zhu, W. and Gao, L. (2014a) Analysis of cell concentration, volume concentration,
448 and colony size of *Microcystis* via laser particle analyzer. *Environ. Manage.* 53, 947–958.

449 Li, M., Zhu, W., Gao, L. and Lu, L. (2013) Changes in extracellular polysaccharide
450 content and morphology of *Microcystis aeruginosa* at different specific growth rates. *J.*
451 *Appl. Phycol.* 25, 1023–1030.

452 Li, M., Zhu, W., Guo, L., Hu, J., Chen, H. and Xiao, M. (2016) To increase size or
453 decrease density? Different *Microcystis* species has different choice to form blooms. Sci.
454 Rep. 6, 37056.

455 Li, M., Zhu, W. and Sun, Q. (2014b) Solubilisation of mucilage induces changes in
456 *Microcystis* colonial morphology. New Zeal. J. Mar. Fresh. 48, 38–47.

457 Lilindenschmidt, K.E. (1999) Controlling the growth of *Microcystis* using surged artificial
458 aeration. Int. Rev. Hydrobiol. 84, 243–254.

459 MacKenzie, B. and Leggett, W. (1993) Wind-based models for estimating the dissipation
460 rates of turbulent energy in aquatic environments: empirical comparisons. Mar. Ecol.
461 Prog. Ser. 94, 207–216.

462 O'Brien, K.R. (2003) The effects of turbulent mixing on the vertical distribution and
463 biomass of phytoplankton populations, University of Western Australia.

464 O'Brien, K.R., Meyer, D.L., Waite, A.M., Ivey, G.N. and Hamilton, D.P. (2004)
465 Disaggregation of *Microcystis aeruginosa* colonies under turbulent mixing: laboratory
466 experiments in a grid-stirred tank. Hydrobiologia 519, 143–152.

467 Oliver, R.L., Hamilton, D.P., Brookes, J.D. and Ganf, G.G. (2012) Ecology of
468 Cyanobacteria II, pp. 155–194, Springer.

469 Otsuka, S., Suda, S., Li, R., Matsumoto, S. and Watanabe, M.M. (2000) Morphological
470 variability of colonies of *Microcystis* morphospecies in culture. J. Gen. Appl. Microbiol.
471 46, 39–50.

472 Otsuka, S., Suda, S., Li, R., Watanabe, M., Oyaizu, H., Matsumoto, S. and Watanabe,
473 M.M. (1998) 16S rDNA sequences and phylogenetic analyses of *Microcystis* strains with
474 and without phycoerythrin. FEMS Microbiol. Lett. 164, 119–124.

475 Otsuka, S., Suda, S., Li, R., Watanabe, M., Oyaizu, H., Matsumoto, S. and Watanabe,
476 M.M. (1999) Phylogenetic relationships between toxic and non-toxic strains of the genus
477 *Microcystis* based on 16S to 23S internal transcribed spacer sequence. FEMS Microbiol.
478 Lett. 172, 15–21.

479 Otsuka, S., Suda, S., Shibata, S., Oyaizu, H., Matsumoto, S. and Watanabe, M.M. (2001)
480 A proposal for the unification of five species of the cyanobacterial genus *Microcystis*
481 Kutzing ex Lemmermann 1907 under the rules of the Bacteriological Code. Int. J. Syst.
482 Evol. Microbiol. 51, 873–879.

483 Otten, T.G. and Paerl, H.W. (2011) Phylogenetic inference of colony isolates comprising
484 seasonal *Microcystis* blooms in Lake Taihu, China. Microb. Ecol. 62, 907–918.

485 Ozawa, K., Fujioka, H., Muranaka, M., Yokoyama, A., Katagami, Y., Homma, T.,
486 Ishikawa, K., Tsujimura, S., Kumagai, M., Watanabe, M.F. and Park, H.D. (2005) Spatial
487 distribution and temporal variation of *Microcystis* species composition and microcystin
488 concentration in Lake Biwa. Environ. Toxicol. 20, 270–276.

489 Park, H.D., Watanabe, M.F., Harada, K.I., Suzuki, M., Hayashi, H. and Okino, T. (1993)
490 Seasonal variations of *Microcystis* species and toxic heptapeptide microcystins in Lake
491 Suwa. Environ. Toxicol. Water Qual. 8, 425–435.

492 Peters, F. and Marrasé, C. (2000) Effects of turbulence on plankton: an overview of
493 experimental evidence and some theoretical considerations. Mar. Ecol. Prog. Ser. 205,
494 291–306.

495 Pfeifer, F. (2012) Distribution, formation and regulation of gas vesicles. Nat. Rev.
496 Microbiol. 10, 705–715.

497 Regel, R.H., Brookes, J.D., Ganf, G.G. and Griffiths, R.W. (2004) The influence of

498 experimentally generated turbulence on the Mash01 unicellular *Microcystis aeruginosa*
499 strain. *Hydrobiologia* 517, 107–120.

500 Rowe, M., Anderson, E., Wynne, T., Stumpf, R., Fanslow, D., Kijanka, K., Vanderploeg,
501 H., Strickler, J. and Davis, T. (2016) Vertical distribution of buoyant *Microcystis* blooms
502 in a Lagrangian particle tracking model for short-term forecasts in Lake Erie. *J. Geophys.*
503 *Res. Oceans* 121, 5296–5314.

504 Tan, W., Liu, Y., Wu, Z., Lin, S., Yu, G., Yu, B. and Li, R. (2010) *cpcBA-IGS* as an
505 effective marker to characterize *Microcystis wesenbergii* (Komárek) Komárek in
506 *Kondrateva* (cyanobacteria). *Harmful Algae* 9, 607–612.

507 Tsukada, H., Tsujimura, S. and Nakahara, H. (2006) Seasonal succession of
508 phytoplankton in Lake Yogo over 2 years: effect of artificial manipulation. *Limnology* 7,
509 3–14.

510 Visser, P.M., Ibelings, B.W., Bormans, M. and Huisman, J. (2016) Artificial mixing to
511 control cyanobacterial blooms: a review. *Aquatic Ecol.* 50, 423–441.

512 Visser, P.M., Ibelings, B.W., van der Veer, B., Koedood, J. and Mur, L.R. (1996) Artificial
513 mixing prevents nuisance blooms of the cyanobacterium *Microcystis* in Lake Nieuwe
514 Meer, the Netherlands. *Freshw. Biol.* 36, 435–450.

515 Wallace, B.B., Bailey, M.C. and Hamilton, D.P. (2000) Simulation of vertical position of
516 buoyancy regulating *Microcystis aeruginosa* in a shallow eutrophic lake. *Aquat. Sci.* 62,
517 320–333.

518 Watanabe, M. (1996) Isolation, cultivation and classification of bloom-forming
519 *Microcystis* in Japan. *Toxic Microcystis* 2, 13–34.

520 Wilkinson, A., Hondzo, M. and Guala, M. (2016) Effect of small-scale turbulence on the

521 growth and metabolism of *Microcystis aeruginosa*. Adv. Microbiol. 6, 351–367.

522 Wüest, A. and Lorke, A. (2003) Small-scale hydrodynamics in lakes. Annu. Rev. Fluid
523 Mech. 35, 373–412.

524 Xiao, M., Li, M. and Reynolds, C.S. (2018) Colony formation in the cyanobacterium
525 *Microcystis*. Biol. Rev. Camb. Philos. Soc. Doi: 10.1111/brv.12401.

526 Xiao, Y., Li, Z., Li, C., Zhang, Z. and Guo, J. (2016) Effect of small-scale turbulence on
527 the physiology and morphology of two bloom-forming cyanobacteria. PLoS ONE 11,
528 e0168925.

529 Xu, S., Peng, Q. and Li, M. (2014) Morphospecies and genospecies of *Microcystis* during
530 blooms in eutrophic Lake Taihu (China) in autumn. Biochem. Syst. Ecol. 57, 322–327.

531 Xu, S., Sun, Q., Zhou, X., Tan, X., Xiao, M., Zhu, W. and Li, M. (2016) Polysaccharide
532 biosynthesis-related genes explain phenotype-genotype correlation of *Microcystis*
533 colonies in Meiliang Bay of Lake Taihu, China. Sci. Rep. 6, 35551.

534 Yamamoto, Y. and Nakahara, H. (2009) Seasonal variations in the morphology of bloom-
535 forming cyanobacteria in a eutrophic pond. Limnology 10, 185–193.

536 Yang, Z., Kong, F., Shi, X., Zhang, M., Xing, P. and Cao, H. (2008) Changes in the
537 morphology and polysaccharide content of *Microcystis aeruginosa* (Cyanobacteria)
538 during flagellate grazing. J. Phycol. 44, 716–720.

539 Yu, G., Song, L. and Li, R. (2007) Taxonomic notes on water bloom forming *Microcystis*
540 *species* (Cyanophyta) from China-an example from samples of the Dianchi lake. Acta
541 Phytotaxonomica Sinica 45, 727–741. (Chinese with English Abstract).

542 Zhang, G., Zhang, P., Wang, B. and Liu, H. (2006) Ultrasonic frequency effects on the
543 removal of *Microcystis aeruginosa*. Ultrason. Sonochem. 13, 446–450.

544 Zhang, P., Galindo-Torres, S., Tang, H., Jin, G., Scheuermann, A. and Li, L. (2017) An
545 efficient Discrete Element Lattice Boltzmann model for simulation of particle-fluid,
546 particle-particle interactions. *Comput. Fluids* 147, 63–71.

547 Zhang, P., Galindo-Torres, S.A., Tang, H., Jin, G., Scheuermann, A. and Li, L. (2016)
548 Lattice Boltzmann simulations of settling behaviors of irregularly shaped particles. *Phys.*
549 *Rev. E* 93, 062612.

550 Zhou, J., Qin, B., Han, X. and Zhu, L. (2016) Turbulence increases the risk of
551 microcystin exposure in a eutrophic lake (Lake Taihu) during cyanobacterial bloom
552 periods. *Harmful algae* 55, 213–220.

553 Zhu, W., Li, M., Luo, Y., Dai, X., Guo, L., Xiao, M., Huang, J. and Tan, X. (2014)
554 Vertical distribution of *Microcystis* colony size in Lake Taihu: its role in algal blooms. *J.*
555 *Great Lakes Res.* 40, 949–955.

556 Zhu, W., Zhou, X., Chen, H., Gao, L., Xiao, M. and Li, M. (2016) High nutrient
557 concentration and temperature alleviated formation of large colonies of *Microcystis*:
558 evidence from field investigations and laboratory experiments. *Water Res.* 101, 167–175.
559

560 **Tables**

561 Table 1: Turbulent kinetic energy (TKE, $\text{m}^2 \text{s}^{-2}$), turbulent dissipation rate ($\text{m}^2 \text{s}^{-3}$) and
 562 Kolmogorov microscale (μm) at the six rotation speeds, estimated by the computational
 563 fluid dynamics (CFD) hydrodynamic model (Discrete Element Lattice Boltzmann
 564 Method, DELBM).

Experiment	1	2	3	4	5	6
Speed of the propeller (rpm)	600	800	1000	1200	1400	1600
Turbulent kinetic energy ($\text{m}^2 \text{s}^{-2}$)	0.0030	0.0053	0.0083	0.0117	0.0157	0.0206
Turbulent dissipation rate ($\text{m}^2 \text{s}^{-3}$)	0.020	0.048	0.094	0.155	0.241	0.364
Kolmogorov microscale (μm)	83.6	67.5	57.1	50.3	45.1	40.7

565

566 **Figure captions**

567 Fig. 1: (a) Schematic of the beaker and propeller used to mix *Microcystis* samples and the
568 laser particle analyzer used to measure colony size distribution. The propeller is described
569 by three-dimensional polygon meshes using a Computed Tomography (CT) scan to
570 minimize numerical shape differences between simulations and the observed set-up. (b –
571 g) Steady-state total turbulent kinetic energy (TKE, $\text{m}^2 \text{s}^{-2}$) under the six rotation speeds:
572 a. 600 rpm; b. 800 rpm; c. 1000 rpm; d. 1200 rpm; e. 1400 rpm; and f. 1600 rpm. Units
573 for the stirring device are mm, and color bar from blue to red indicates the magnitude of
574 dimensionless velocity, increasing from 0 to 0.100.

575 Fig. 2: D_{50} (50% of the population is smaller than this size) of colonies (μm) during the
576 30-min mixing of the three *Microcystis* morphospecies. a, small *M. ichthyoblabe* colony;
577 b, small *M. wesenbergii* colony; c, small *M. aeruginosa* colony; d, medium
578 *M. ichthyoblabe* colony; e, medium *M. wesenbergii* colony; f, medium *M. aeruginosa*
579 colony; g, large *M. ichthyoblabe* colony; h, large *M. wesenbergii* colony; i, large
580 *M. aeruginosa* colony. Dots in different colours showed the six different rotation speeds.

581 Fig. 3: Relationship between D_{50} of the three size groups of the three *Microcystis*
582 morphospecies after 30-min mixing against the Kolmogorov scale (μm). The
583 Kolmogorov scale was simulated by the DELBM model under the six rotation speeds. a,
584 *M. ichthyoblabe*; b, *M. wesenbergii*; and c, *M. aeruginosa*. The initial D_{50} (μm) values for
585 each sieved size groups were marked for each morphospecies. Slope = 1 corresponds to
586 the minimum size of disaggregated colonies and is similar to the Kolmogorov scale (μm).

587 Fig. 4: Photomicrographs of *M. ichthyoblabe*, *M. aeruginosa* and *M. wesenbergii*
588 colonies before and after mixing treatments (a – f). a, initial *M. ichthyoblabe* colonies; b,

589 *M. ichthyoblabe* colonies after 30-min mixing; c, initial *M. aeruginosa* colonies; d,
590 *M. aeruginosa* colonies after 30-min mixing; e, initial spherical *M. wesenbergii*; f,
591 transitional *M. wesenbergii* colonies; and g, reticular *M. wesenbergii* colonies after 30-
592 min mixing. The scale bar was marked for all photomicrographs, as 200 μm .

593 Fig. 5: Volume proportion of colonies in different morphologies before (control) and after
594 the mixing experiments of *M. wesenbergii* colonies under the six turbulent dissipation
595 rates. a – c were the small, medium and large size groups.

596 Fig. 6: Conceptual model of morphological changes in *M. wesenbergii*-like colonies to
597 *M. aeruginosa*-like colonies.

Figures

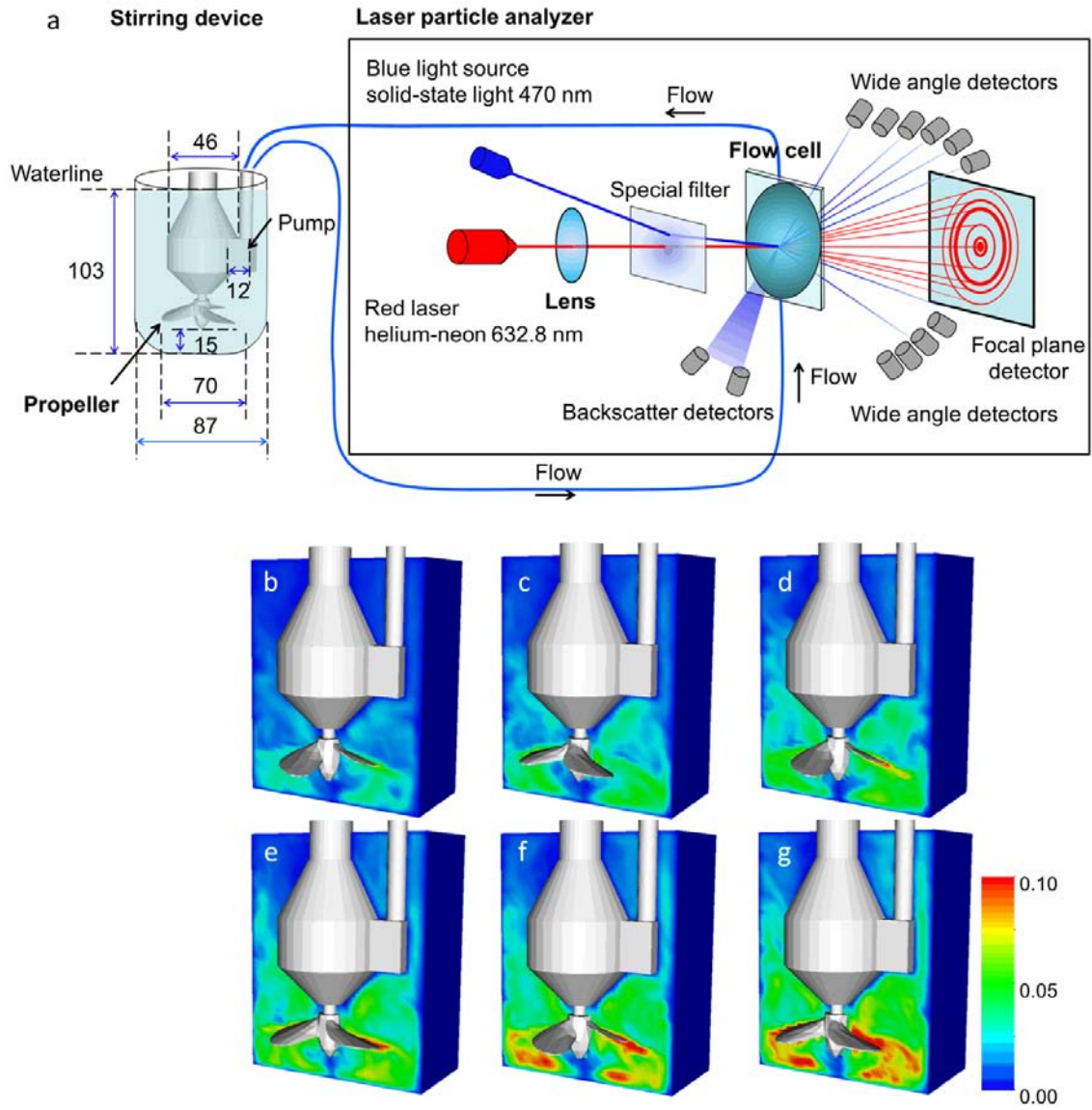


Fig. 1

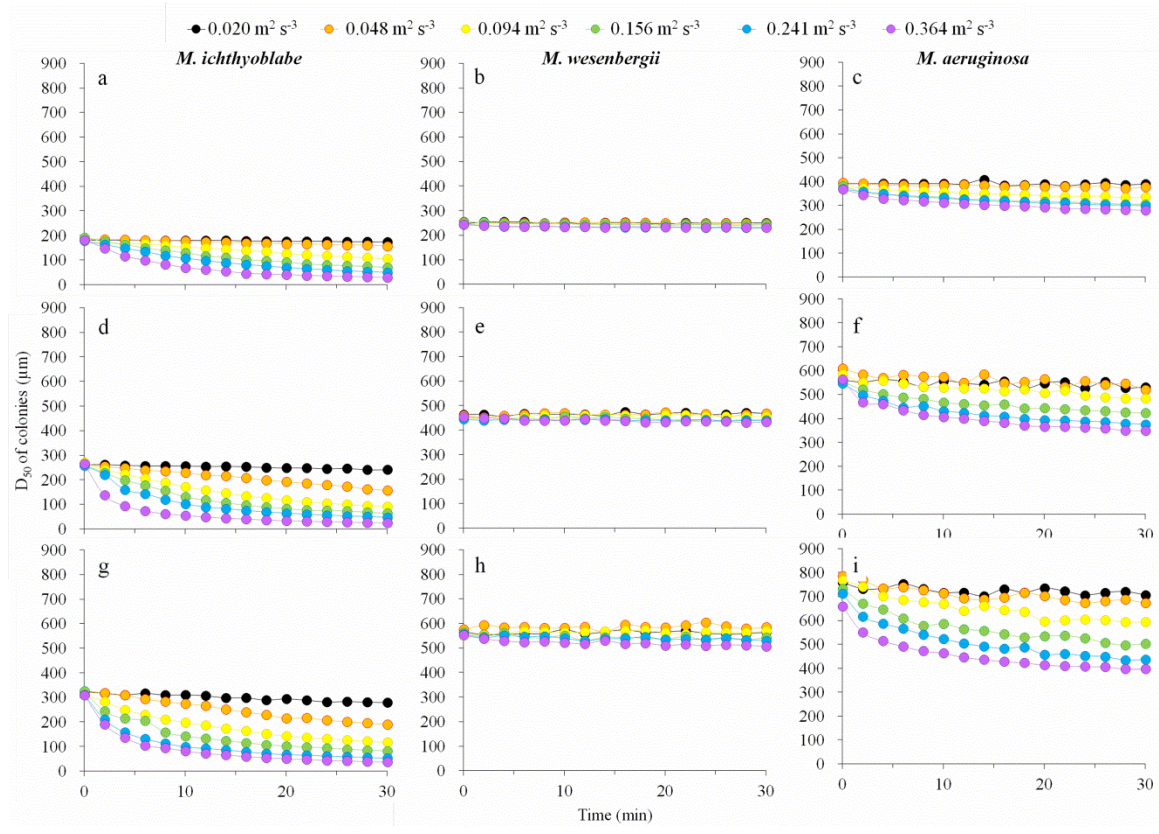


Fig. 2

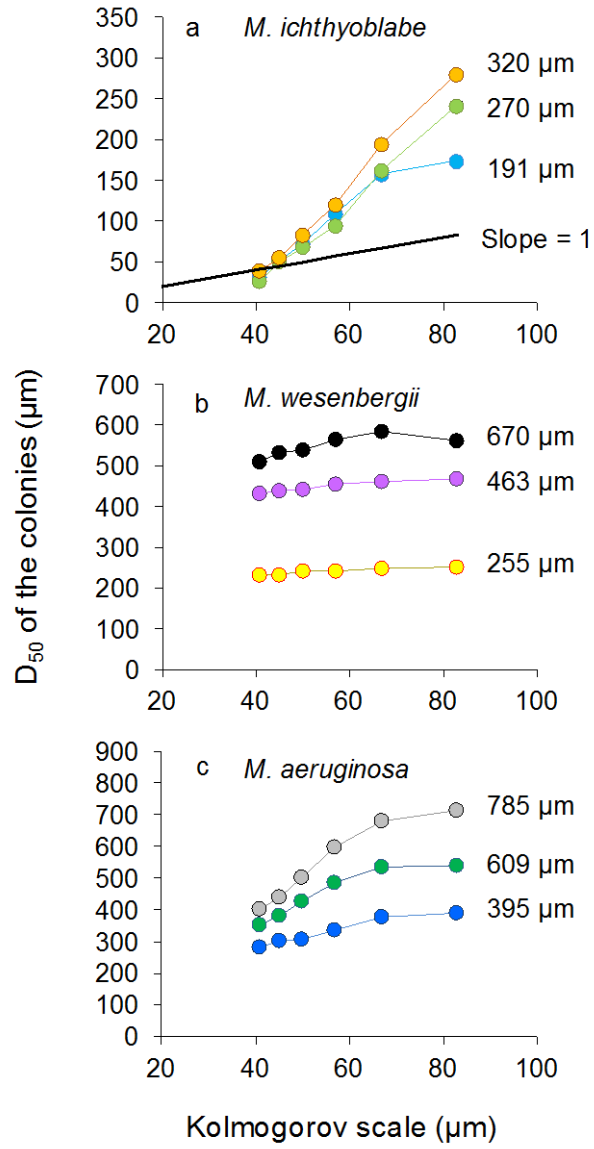


Fig. 3

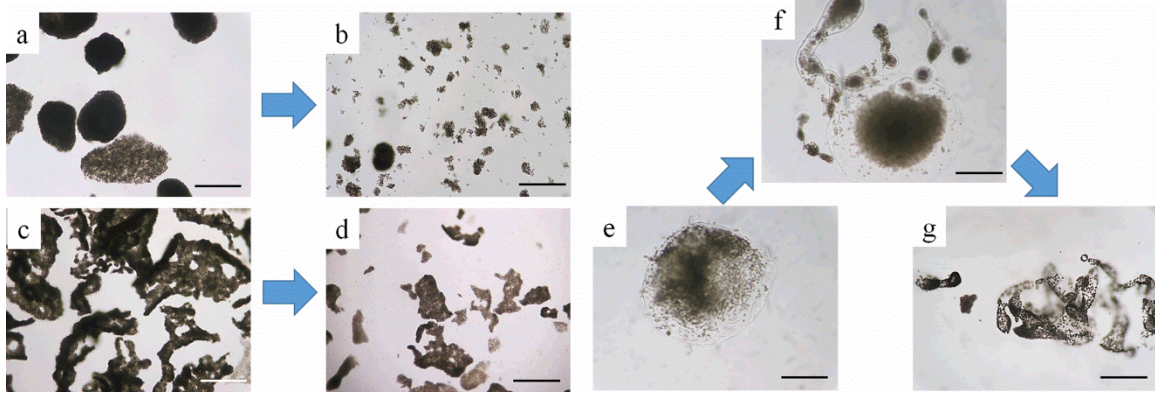


Fig. 4

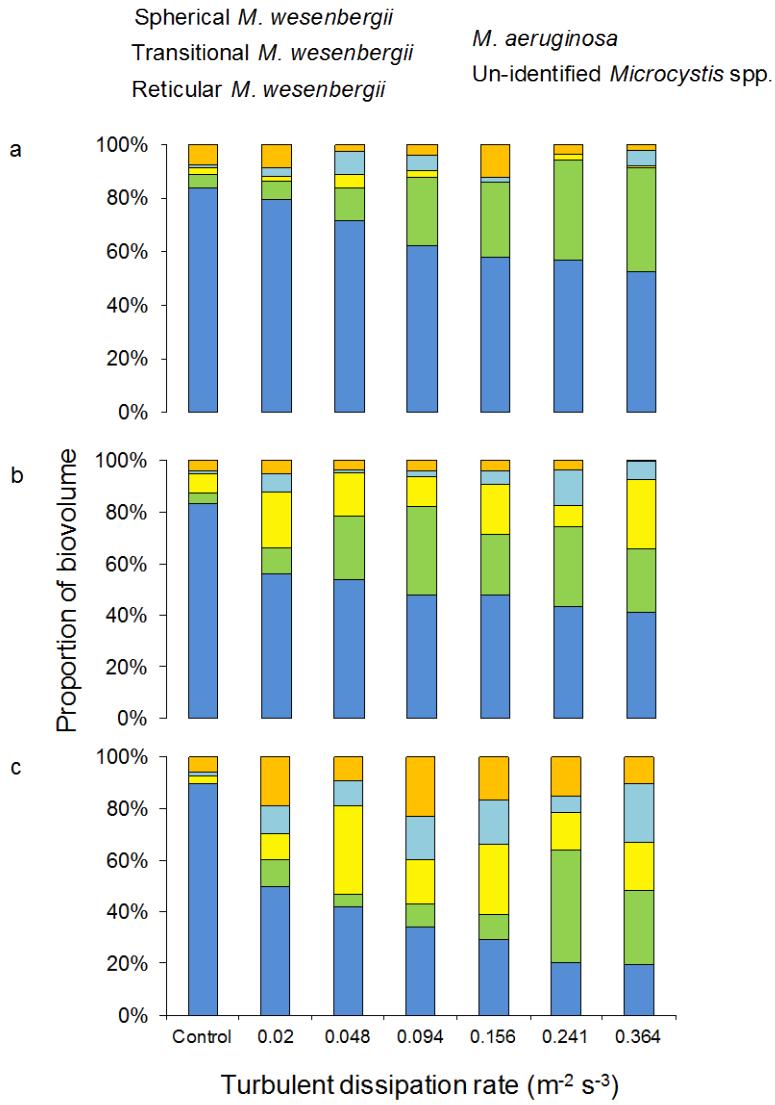


Fig. 5

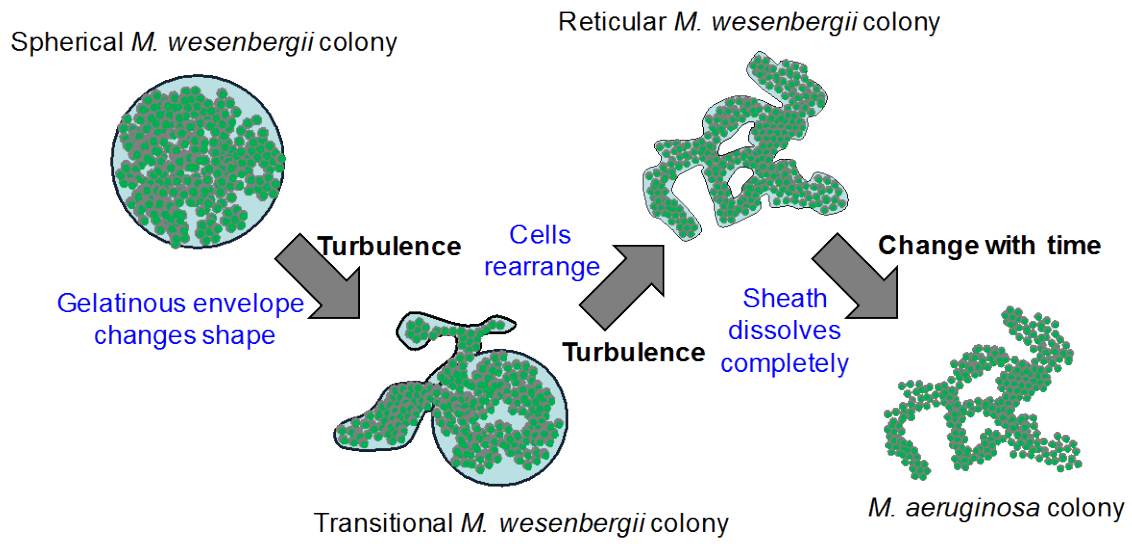


Fig. 6